ELSEVIER

Polymer 44 (2003) 1295–1307

polymer

www.elsevier.com/locate/polymer

Compatibilisation of heterogeneous acrylonitrile–butadiene rubber/polystyrene blends by the addition of styrene–acrylonitrile copolymer: effect on morphology and mechanical properties

Monsy Mathew, Sabu Thomas*

School of Chemical Sciences, Mahatma Gandhi University, Priyadarsini Hills PO, Kottayam 686 560, Kerala, India

Received 2 August 2001; received in revised form 17 May 2002; accepted 31 May 2002

Abstract

Compatibility of polystyrene (PS) and acrylonitrile–butadiene rubber (NBR) blend is poor, hence technological compatibilisation was sought by the addition of styrene–acrylonitrile copolymer (SAN). The interfacial activity of SAN was studied as a function of compatibiliser concentration by following the morphology of three different blend series, viz. PS/NBR 30/70, 50/50 and 70/30. Incorporation of SAN into PS/NBR blends improved tensile, tear, hardness and impact properties. Addition of SAN beyond the saturation level (critical micelle concentration) adversely affected the ultimate properties. Attempts were made to understand the conformation of the compatibiliser at the interface. The protocol of mixing was varied, and, its effect on the mechanical properties was investigated. The experimental results were compared with the theoretical predictions of Noolandi and Hong.

Keywords: Polymer blends; Compatibilisation; Nitrile rubber

1. Introduction

The advent of polymer melt-blending technique has certainly provided an easy and efficient way to generate new high-performance materials, starting from largely available monomers and polymers. Among the different type of polymer blends, thermoplastic elastomer blends (TPEs) combine the excellent processing characteristics of the thermoplastics at high temperatures with the resilience and flexibility associated with vulcanised elastomers at the service temperature [1,2]. Even though blending is an easy method for the preparation of TPEs, most of the blends are immiscible and exhibit poor mechanical properties. In such heterogeneous systems, a satisfactory over-all physico-mechanical behaviour will critically depend on two demanding structural parameters: a proper interfacial tension leading to a phase size small enough to allow the material to be considered as macroscopically homogeneous and an interface adhesion strong enough to assimilate stresses and strains without disruption of the established morphology [3].

Blends of acrylonitrile–butadiene rubber (NBR) and polystyrene (PS) are an interesting class of thermoplastic elastomers, which would combine the excellent oil-resistant properties of NBR and the superior mechanical and processing characteristics of PS. NBR compounds assume commercial interest due to its excellent oil-resistance, abrasion resistance and elastic properties. However, it shows poor ozone resistance. Several polymers have been blended with NBR to make high performance oil-resistant and gas-barrier products [4–6]. PS offers excellent ozone resistance, weather resistance, mechanical properties and easy processability. Unfortunately, blends of NBR and PS form incompatible mixtures, owing to the poor interaction between the two constituent polymers [7]. Till date, no serious effort have been made to develop a technologically compatible and viable TPE of NBR and PS. Over the years, different techniques have been developed to alleviate the problem of incompatibility in blends [8]. These include (i) the addition of a third homopolymer or graft or block copolymer which is miscible with the two phases, and (ii) the introduction of covalent bonds between the homo-polymer phases. The first one can be considered as non-reactive compatibilisation, and, is made use of in our work. The addition of these interfacial agents or compatibilisers reduce the surface tension between the phases and thereby improve the interfacial adhesion and mechanical properties,

* Corresponding author. Tel.: +91-481-598-303; fax: +91-481-561-190.
E-mail address: sabut@md4.vsnl.net.in (S. Thomas).

0032-3861/03/$ - see front matter © 2002 Published by Elsevier Science Ltd.
PII: S0032-3861(02)00356-7

Table 1
Details of materials used

Materials	Characteristics[a]		Source
Nitrile rubber (Aparene N553NS)	Volatile matter (%)	0.130	Gujarat Apar Polymer Ltd, Mumbai
	Antioxidant (%)	1.400	
	Organic acid (%)	0.250	
	Soap (%)	0.004	
	Mooney viscosity, ML_{1+4} 100 °C	40.00	
	Bound –CN (wt%)	34.00	
	Density	0.911 g/cm^3	
	Mol. wt ($\bar{M}_w$)	13.49×10^4 g/mol	
Polystyrene (atactic)	Density	1.021 g/cm^3	Polychem India Pvt. Ltd, Mumbai
	Mol. wt ($\bar{M}_w$)	10.62×10^4 g/mol	
Styrene–acrylonitrile (random)	Density	1.087 g/cm^3	Anoopam Plastics India Ltd, New Delhi
	–CN (wt%)	24.00	
	Mol. wt ($\bar{M}_w$)	15.59×10^4 g/mol	

[a] Composition of additives are expressed in wt%.

even when used in rather low proportions. There are several studies in literature in which addition of tailored copolymer as interfacial agent increases the compatibility of immiscible polymer pairs [9–16]. The thermodynamic theories concerning the emulsifying effect of copolymer in heterogeneous polymer blends have been developed by Leibler for semi-compatible blends [17,18], and Noolandi and Hong for immiscible blends [19,20]. According to the two theories, the localisation of the compatibiliser at the interface results in broadening of the interface between the homopolymers and lowering of the interaction energy between the two immiscible homopolymers.

In the present study, the effect of styrene–acrylonitrile copolymer (SAN) as a potential compatibiliser for PS/NBR blends was investigated. The effect of this compatibilisation on the morphology, processing characteristics and mechanical properties was also studied.

2. Experimental

2.1. Materials and blend preparation

The following polymers were used in the work: PS (atactic), NBR (–CN content: 34%), and styrene-*co*-acrylonitrile copolymer (–CN content: 24%). The details and the source of the polymers are given in Table 1. The mixtures are denoted by PS_{100},PS_{70},…,PS_0 corresponding to the weight percentage of PS in the blends. The incorporated SAN content are denoted by S_{10},S_5,…,S_0 corresponding to the weight percentage of SAN in the blends. For preparing solution-casted blends, a 5% (w/v) of PS/NBR/SAN mixture in the required proportion was soaked in chloroform and stirred for 24 h. The solution was casted on a glass plate and dried in a vacuum oven at 110 °C for 48 h. For preparing melt-mixed blends, the components were melt-blended using a Brabender Plasticorder (PLE 331). The torque and temperature evolution with time for melting operation was monitored in the plasticorder. The mixer was operated at 180 °C, maintaining the rotor speed at 60 rpm. At the start, PS was allowed to soften for 2 min and NBR was added thereafter. The SAN was incorporated at the fourth minute of the mixing cycle. The total mixing time of all blends were 6 min in all the cases. The molten mix was quickly removed from the chamber and the hot mixes were subsequently pressed into plaques. Plaques were compression-moulded at 190 °C for 10 min into sheets of 2 mm thickness in a preheated hydraulic press.

2.2. Testing procedure

The test specimens were cut from the solution-casted or melt-mixed sheets using appropriate punching dies. All the specimens were subjected to vacuum drying to remove the moisture. The densities of the polymeric specimens were determined using immersion technique with a 'density determination kit' (Mettler-3360). The non-solvent methanol was used as the auxiliary liquid, and utmost care was taken to avoid air-bubbles adhering to the submerged test specimens. The tensile testing of the samples was performed according to ASTM D 412-80 method using dumb-bell shaped test specimens at a crosshead speed of 50 mm/min using a Universal testing machine (Zwick 1465). The tear strength was determined as per ASTM D 624-81 method using un-nicked 90° angle test pieces, at a strain rate of 50 mm/min. Hardness was measured according to ASTM D 2240-81 method, using a shore D durometer. The Izod impact strength was determined with a Resilience test pendulum impact-tester (ATS FAAR IMPACT-15) using rectangular test specimens as per ASTM D 256 test method. Using a standard cutter, notches were cut in the test pieces at an angle of 45° with radius of the top of the notch being 0.25 mm. All the above tests were performed at 28 ± 1 °C. All the reported results here were averaged from a minimum of six tests. The blend microstructure was analysed by scanning electron microscopy. The compression-moulded

Table 2
Mechanical properties of uncompatibilised PS/NBR blends

Sample	Prep. method[a]	Steady torque[b] (N m)	Young's modulus (MPa)	Stress-at-break (MPa)	Break-strain (%)	Tear strength (N/mm)	Notched Izod impact strength (J/m)
PS_0	Sol-mix	–	1.5 ± 0.3	0.62 ± 0.2	408 ± 7	0.8 ± 0.2	n.d.
PS_{30}	Sol-mix	–	6.7 ± 2.3	3.5 ± 0.6	131 ± 11	13.9 ± 0.1	n.d.
PS_{50}	Sol-mix	–	80.6 ± 7.0	10.6 ± 0.6	40.5 ± 2.5	52.3 ± 0.2	n.d.
PS_{70}	Sol-mix	–	240 ± 10	19.2 ± 0.8	19.5 ± 0.5	74.3 ± 0.6	n.d.
PS_{100}	Sol-mix	–	290 ± 13	12.3 ± 0.5	5.9 ± 0.4	12.8 ± 0.7	n.d.
PS_0	Melt-mix	14.1	1.3 ± 0.4	0.35 ± 0.1	394 ± 5	0.65 ± 0.1	n.d.
PS_{30}	Melt-mix	10.3	3.6 ± 1.6	1.3 ± 0.3	119 ± 11	7.9 ± 0.1	514 ± 2.9
PS_{50}	Melt-mix	8.6	50.6 ± 17	5.5 ± 0.6	21.8 ± 2.5	39.5 ± 0.2	625 ± 18
PS_{70}	Melt-mix	6.3	125 ± 10	14.2 ± 0.8	9.8 ± 0.5	56.3 ± 0.6	110 ± 2.5
PS_{100}	Melt-mix	6.0	186 ± 6.3	7.8 ± 0.1	5.5 ± 0.3	10.5 ± 0.4	20 ± 0.7

Values are mean standard deviation; n.d.: not done.
[a] Sol-mix: solution-casted (chloroform) blends; melt-mix: melt-mixed blends.
[b] Equilibrium torque value at the end of the melt-mixing process.

sheets of the blends were fractured in liquid nitrogen. After the fracturing, the PS-phase was preferentially etched out using cyclohexane for facilitating the phase identification. The dried samples were sputter coated with gold and examined in a JEOL JSM-35C scanning electron microscope (SEM). The morphology of the solution-casted samples was observed with an optical microscope (Leitz Orthoplan). The particle size measurements were performed using an image analyser (Projectina). The number average radius, $\bar{R}_n$ and the weight average radius, $\bar{R}_w$ of the dispersed domain phases in the blends are defined as follows [21]: $\bar{R}_n = (\sum n_i R_i)/\sum n_i$; $\bar{R}_w = (\sum n_i R_i^4)/(\sum n_i R_i^3)$. The polydispersity index (PDI) is defined as $\bar{R}_w/\bar{R}_n$ [21]. The average particle size and particle size distribution reported represent the contribution from at least 300 particles measured for each blend.

3. Results and discussion

3.1. Uncompatibilised PS/NBR blends

From the mechanical properties listed in Table 2, the PS/NBR blends show essentially negative deviation from the additive contribution of each component, suggesting poor interfacial adhesion [22]. The PS_{70} has moderate stress-at-break and break-strain values. The PS_{30} is typically elastomeric, with a low stress-at-break and a very high break-strain. The ultimate tear strength of blends exhibited synergistic positive deviation, higher than even virgin PS. The Izod impact strength of PS/NBR blends decreases with the addition of PS beyond 50%. The poor mechanical properties indicate that PS/NBR blends are incompatible.

3.2. Compatibilisation with random SAN copolymer

A favourable intermolecular interaction between SAN–PS and SAN–NBR pair is expected due to their structural similarity. Hence, random SAN copolymer is a logical choice as a compatibiliser in PS/NBR blends. Due to the close affinity of the styrene segments towards the PS-phase and the acrylonitrile segments towards the NBR-phase, the localisation of SAN molecules at the interface is increasingly favoured. This would facilitate the effective dissipation of stress from the matrix to dispersed phase, thereby, increasing the interfacial strength of the blends.

3.3. Solution-casted blends

The solution-casted PS/NBR blends have been found to be grossly incompatible [22]. The morphology of the compatibilised samples shows that the homogeneity of the blend is drastically improved by the addition of SAN copolymer. The optical micrographs of PS_{30}, PS_{50} and PS_{70} blends with 0 and 5 wt% of SAN are shown in Figs. 1–3, respectively. In the virgin PS_{30} blend, PS phase is dispersed as spherical domains of about 16 μm in diameter in the NBR matrix (Fig. 1(a)). Addition of 5 wt% of SAN in PS_{30} blend reduced the domain size to 6 μm (Fig. 1(b)). In case of PS_{50} blend (Fig. 2(a) and (b)), addition of 5 wt% SAN reduced the dispersed domain size from 27.5 to 0.7 μm. In the PS_{70} blend too, the domain size reduction was very effective from 46 to 1 μm on addition of 5 wt% SAN (Fig. 3). The average size of the dispersed phase is plotted as a function of the weight percentage of SAN copolymer in Fig. 4. The average domain size decreases with increasing concentration of the compatibiliser and finally gets levelled-off at higher concentrations, indicating the gross incompatibility. Addition of only 1 wt% SAN in PS_{50} reduces the domain size from 27.5 to 1.1 μm, i.e. a reduction of 96%. Further additions, corresponding to 2 and 5 wt% SAN caused a reduction of 28 and 10%, respectively. Addition of compatibiliser beyond 5 wt% does not affect any more change in the domain size. The PS_{30} and PS_{70} compatibilised series also show similar trends. The interfaces of all blends seem to be saturated at about 2 wt% SAN

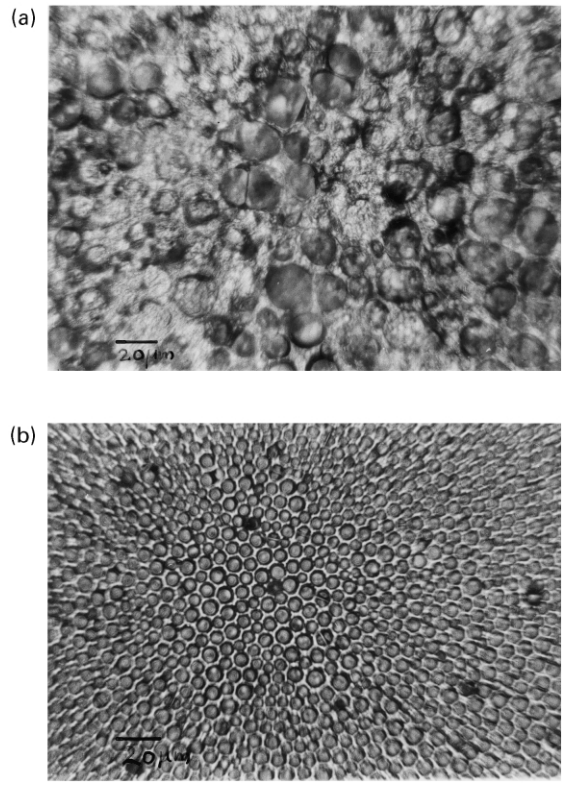

Fig. 1. Optical micrographs illustrating the state of dispersion of PS_{30} blend with (a) 0% SAN; and (b) 5% SAN (solution-casted).

concentration, and no further reduction in domain size was noted at larger amounts.

The equilibrium concentration at which the domain size levelled-off is considered as the 'critical micelle concentration' (CMC). There are numerous published reports on the interfacial saturation by the addition of compatibiliser in heterogeneous blends [17–20]. The pioneering work of Noolandi and Hong predicted that micellar aggregation of the copolymer takes place at the interface of the blend beyond a critical concentration of the copolymer (CMC). According to Noolandi and Hong [19,20], the compatibiliser added to a heterogeneous blend locates at the interface and reduces the interfacial energy by broadening the interfacial area. The consequent reduction in interfacial tension ($\Delta\gamma$) in a heterogeneous binary blend A/B upon the addition of a copolymer A-*b*-B is given by

$$\Delta\gamma = d\phi_c[(1/2\chi + 1/Z_c) - 1/Z_c \exp(Z_c\chi/2)] \quad (1)$$

where d is the width at half height of copolymer profile reduced by Kuhn statistical segment length, χ is the Flory–Huggins interaction parameter between the A and B segment of the AB copolymer, Z_c is the degree of the polymerisation of the copolymer. The theory predicts the proportionality of interfacial tension reduction ($\Delta\gamma$) to copolymer volume fraction (ϕ_c), until the system reaches CMC. However beyond CMC, $\Delta\gamma$ levels-off with ϕ_c. Since interfacial tension reduction is directly proportional to particle size reduction (Δd), it can be substituted for $\Delta\gamma$ in

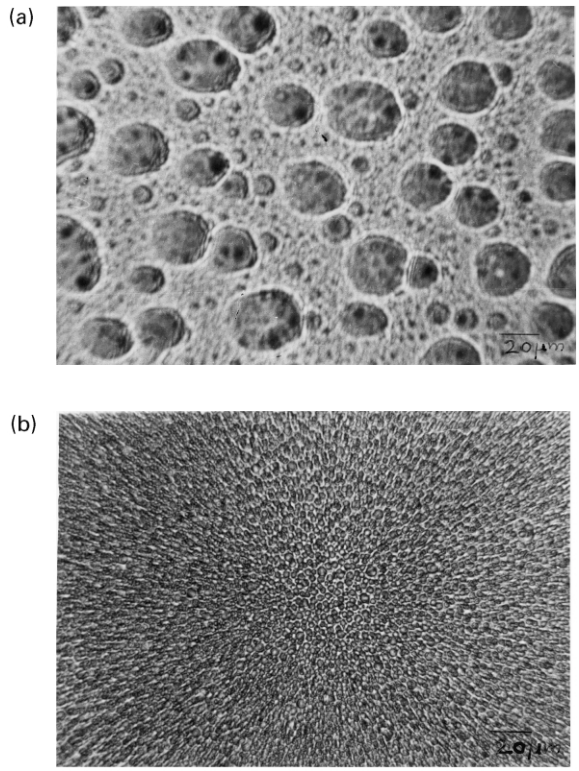

Fig. 2. Optical micrographs illustrating the state of dispersion of PS_{50} blend with (a) 0% SAN; and (b) 5% SAN (solution-casted).

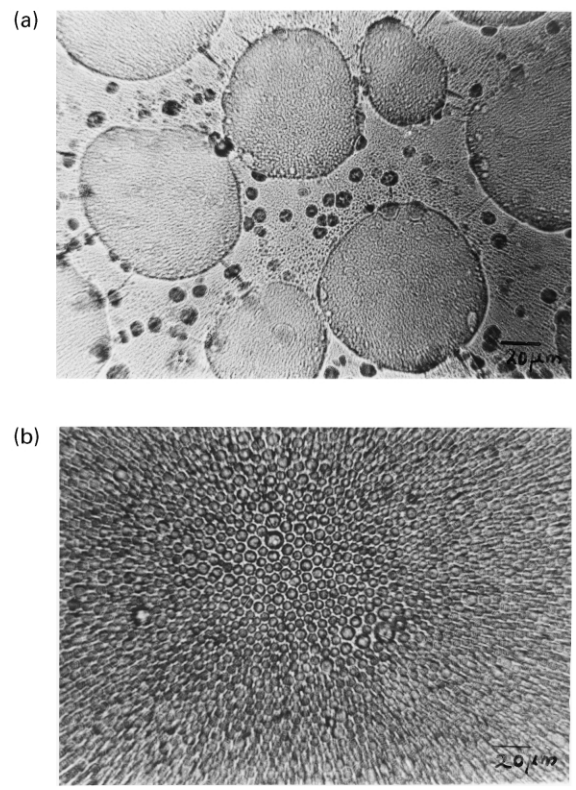

Fig. 3. Optical micrographs illustrating the state of dispersion of PS_{70} blend with (a) 0% SAN; and (b) 5% SAN (solution-casted).

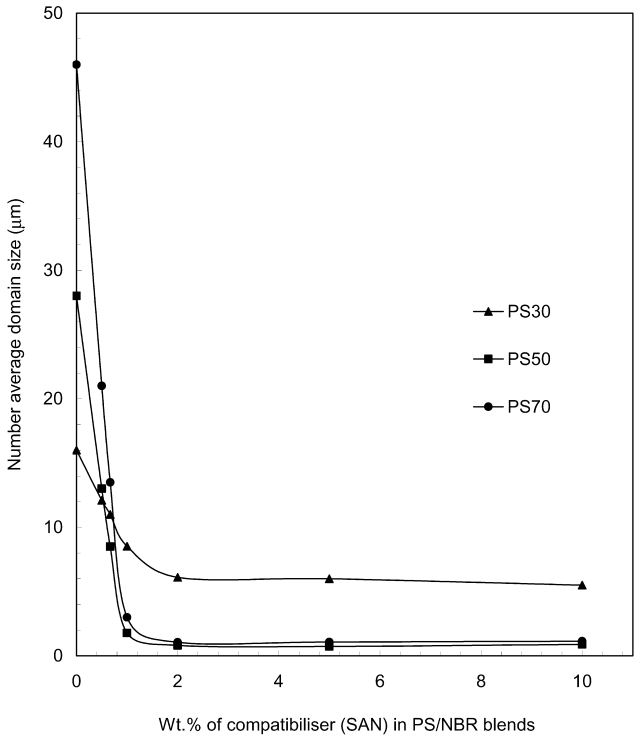

Fig. 4. Effect of compatibiliser (SAN) concentration on the dispersed phase size of solution-casted PS/NBR blends.

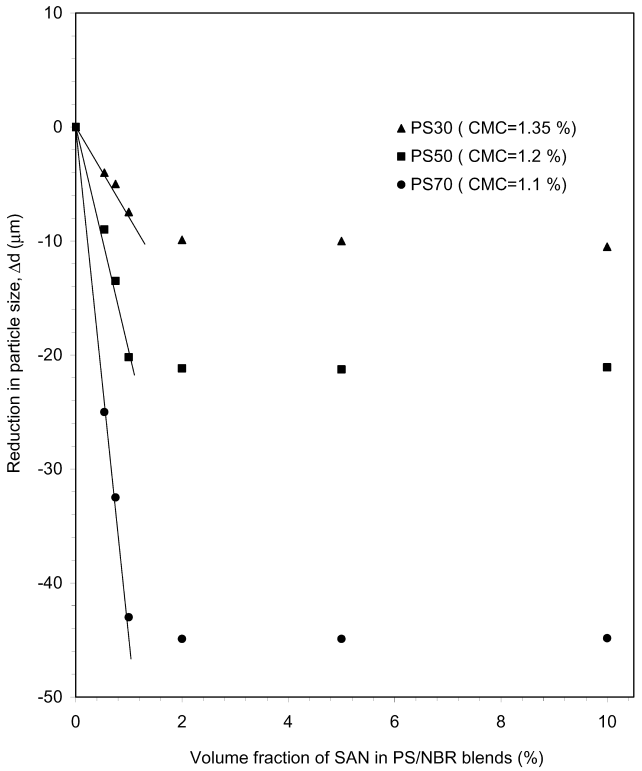

Fig. 5. Effect of percent volume fraction of compatibiliser (SAN) on the domain size reduction of PS/NBR blends.

Eq. (1), and CMC can be determined [16]. Our present work also suggests that there is a critical concentration of the copolymer (i.e. CMC) required to saturate the PS/NBR blend interface. The addition of the compatibiliser beyond this concentration (CMC) leads to undesirable micelle formation, which very often reduces the total performance of the blend system. The plot of Δd versus ϕ_c is given in Fig. 5. It can be seen that at low concentration of the compatibiliser, Δd increases linearly with SAN concentration; and at high loadings, Δd levels-off, as proposed by Noolandi and Hong. The percentage of SAN required to saturate the interface (CMC) was determined, as shown in Fig. 5. Thus, as observed from solution-casted blends, 1.1–1.35% of SAN is sufficient to effectively emulsify the heterogeneous PS/NBR system.

Tang and Huang proposed an equation where the average radius (R) of the dispersed phase is given by [23]

$$R = (R_0 - R_S)\, e^{-KC} + R_S \quad (2)$$

where R_0 and R_S are the average radii of dispersed domains at compatibiliser concentration zero and at saturation, respectively, and C is the concentration of the compatibiliser. The equation is based on the assumption that the change in the interfacial tension with the concentration of compatibiliser is given by

$$-d\gamma/dC = K(\gamma - \gamma_S) \quad (3)$$

where γ is the interfacial tension at a compatibiliser concentration C, γ_S is the interfacial tension at the saturation concentration and K is a constant. The changes of average radii of domains with compatibiliser concentration were fitted to Eq. (2). The fitted parameters for R_n are given in Table 3. The K values are expected to increase with the level of compatibilisation and decrease with the degree of compatibiliser self-association in the blend [21,23]. The addition of SAN not only reduces the domain size but also narrows the size distribution in PS/NBR blends (Fig. 6). The PDI values of the blends are given in Table 4. Addition of SAN in PS/NBR blends narrows the distribution curve and reduces the PDI values. The uncompatibilised blends contained a significantly higher percentage of large domains than the compatibilised ones. The role of a compatibiliser is to lower the interfacial tension and to suppress the coalescence process in blends [24]. The phenomenon of coalescence or aggregation of domains was not noticed in optimally compatibilised blends, as evident from the very small PDI values. Thus, when two domains collide during mixing, a stabilising copolymer layer between the aggregated domains may inhibit coalescence.

The conformation of the compatibiliser at the interface can be predicted based on the interfacial area in the blends. Three different physical models illustrating the conformation of the compatibiliser at the interface are given in literature [16,25,26]. In the fully extended model, the segments are extending into the corresponding homopolymer

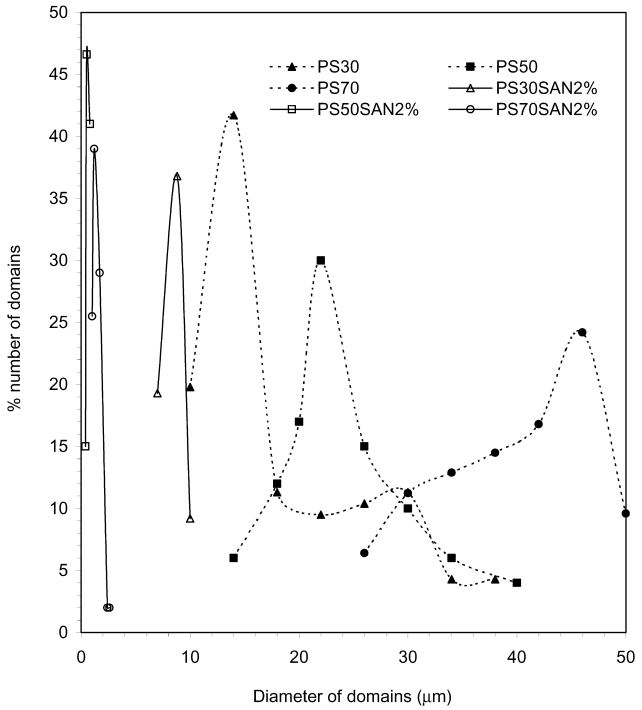

Fig. 6. Domain size distribution of PS/NBR blends with and without compatibiliser (SAN).

phases (Fig. 7(a)). In such a case, the occupied area at the interface is the cross-sectional area of the extended copolymer molecule. In the case of poly(styrene-*co*-acrylonitrile), the theoretical average cross-sectional area of the extended copolymer molecule and, hence, the area it occupies at the interface is $\sim 0.5\,\mathrm{nm}^2$. However, this conformation is unlikely in case of a random copolymer. In the flat model, the occupied copolymer lies almost completely flat at the interface, in which case the occupied area is the lateral surface area of the entire copolymer molecule (Fig. 7(b)). Using the experimental values of root mean square radius of gyration of PS, the lateral surface area of the copolymers were estimated. This is by considering the styrene and acrylonitrile segments of the copolymer as a spherical random coil and calculating the lateral surface area using the experimental values of root mean square radius of gyration of the copolymer, as reported in literature. The lateral surface area of SAN copolymer is approximately

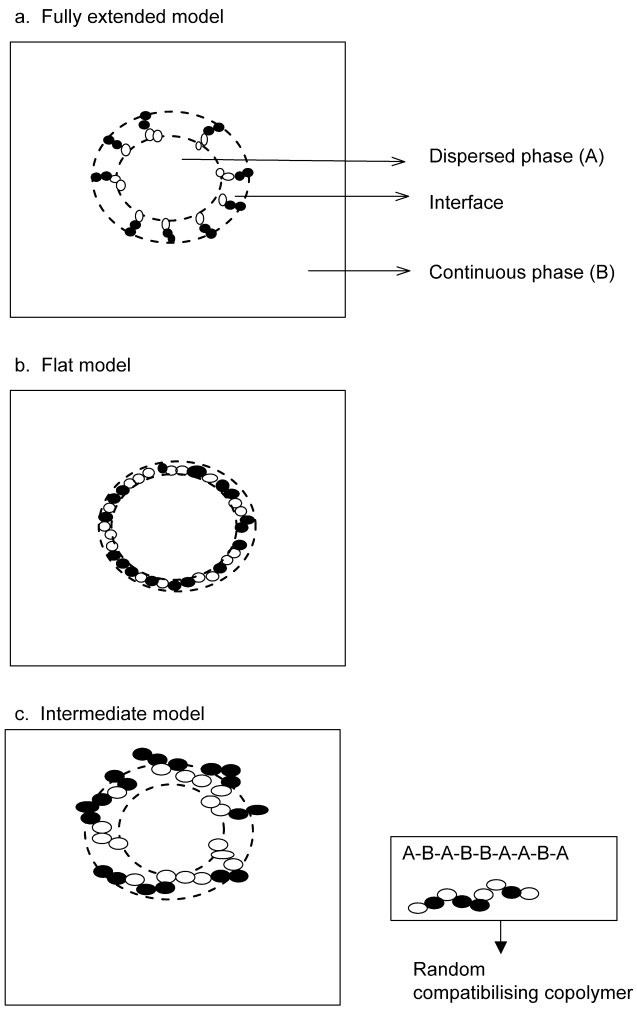

Fig. 7. Speculative models illustrating the possible conformation of the compatibiliser at blend interface: (a) fully extended model; (b) flat model; and (c) intermediate model.

106 nm^2. The area occupied by SAN molecule at the PS/NBR blend interface, Σ, was calculated by using the expression suggested by Paul and Newman [24]

$$\Sigma = \frac{3\phi_A M}{mRN} \tag{4}$$

where M is the molecular weight of the copolymer, N the Avogadro's number, ϕ_A the volume fraction of the

Table 3
K parameter (defined by Eq. (2)) fitted to number-average radii ($\bar{R}_n$) of dispersed domains in PS/NBR 50/50 blend

Wt% of SAN in PS/NBR 50/50 blend	K value
0.50	1.110
0.75	1.359
1.00	3.704
2.00	2.787
5.00	1.392
10.0	0.627

Solution (chloroform) casted blend.

Table 4
Effect of the addition of SAN on the PDI values of solution (chloroform) casted PS/NBR blends

Concentration of SAN in the blend (wt%)	Blend system		
	PS_{30}	PS_{50}	PS_{70}
0	1.15	1.20	1.10
1	1.10	1.04	1.09
2	1.01	1.01	1.02
5	–	1.01	–
10	–	1.03	–

Table 5
Values of interfacial area (Σ) for PS/NBR blends compatibilised with SAN copolymer

Blend system	CMC (%)	Radius at CMC, R (μm)	Σ (nm^2)
PS/NBR (30/70)	1.35	3.07	13.09
PS/NBR (50/50)	1.20	0.44	73.53
PS/NBR (70/30)	1.10	0.55	38.50

Solution (chloroform) casted blends.

homopolymer A in a A/B blend, R the radius of the dispersed domains and m the mass of the copolymer required to saturate unit volume of the blend interface (CMC). The values of interfacial area (Σ) for the blend systems are given in Table 5. The experimental Σ values lie between 13.09 and 73.53 nm^2 for the blends. These values are intermediate between those values obtained from the two models (0.5 and 106 nm^2). This suggests that neither of these models represent the actual situation. The behaviour of a compatibilising random copolymer is intermediate to those of the two models. In such a case, the most realistic conformation of the random copolymer at the interface can be depicted as shown in Fig. 7(c). Due to the attraction of SAN molecules towards both PS and NBR phases, the localisation of the compatibiliser at the interface is favoured. Also, it may be noticed that the area occupied by the SAN molecule at the interface (Σ) is higher for PS_{50} and PS_{70} systems. The PS-rich blends show higher interfacial area than NBR-rich blends. When the low viscous PS is the continuous phase, the interaction between the copolymer and the homopolymers is higher compared to NBR-rich blends. This is because the compatibiliser molecule has higher diffusional mobility when the low viscous PS is the continuous phase. Therefore, it can be easily located at the interface. Greater interaction increases interfacial area (hence high Σ values) and reduces interfacial tension. As the PS content is reduced, the increased viscosity of matrix (NBR) retards the mobility of the copolymer. Hence the amount of copolymer locating at the interface is reduced, resulting in the reduction of interaction between the compatibiliser and the homopolymers. Hence, the area occupied by SAN at the interface (Σ) for PS_{30} (13.09 nm^2) is lower than that of PS_{50} (73.53 nm^2) and PS_{70} (38.50 nm^2).

The increase in interfacial thickness with the addition of SAN in PS/NBR blends is expected to facilitate good interconnection between the phases, thereby, improve the ultimate strength. The stress–strain curves of solution (chloroform) casted blends are shown in Fig. 8(a). There is considerable difference in the deformation behaviour of the compatibilised compositions in comparison to the uncompatibilised ones. The mechanical properties of the solution-casted blends are summarised in Table 6. Improvements in mechanical properties upon the addition of SAN in solution-casted PS/NBR blends (i.e. tensile moduli, stress-at-break, break-strain and tear strength) are evident from the results.

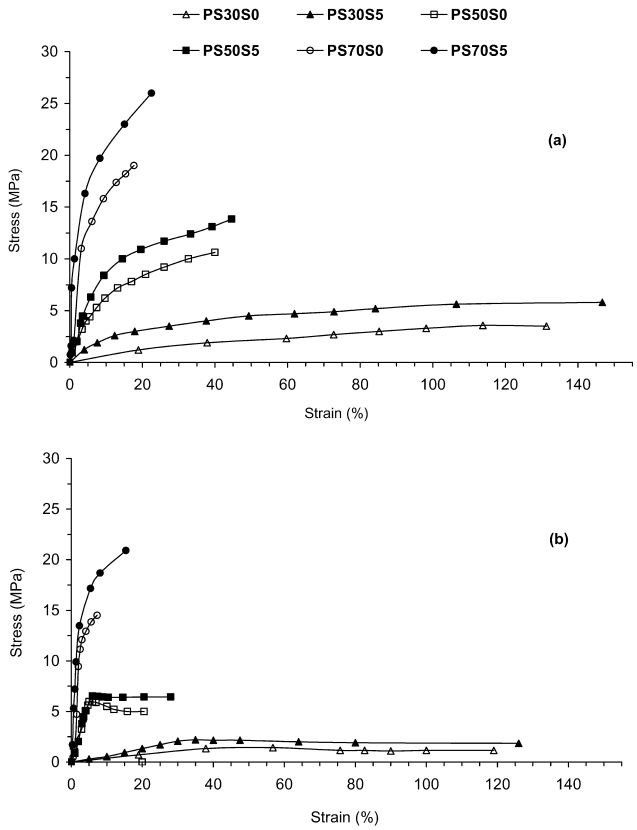

Fig. 8. Tensile stress–strain curves of PS/NBR blends with and without compatibiliser (SAN): (a) solution-casted; and (b) melt-mixed.

The variation of the ultimate properties with the addition of SAN in PS/NBR blends is in agreement with the reduction in size of the dispersed phase. For instance, in Fig. 9, the stress-at-break (σ_b) and the domain size are plotted as a function of SAN concentration. The reduction in domain size and increase in σ_b continue till the interface is saturated. The saturation of PS/NBR 50/50 blend interface by SAN is indicated by the levelling-off of domain size and tensile strength in Fig. 9. The increase in ultimate strength of PS/NBR system upon compatibilisation with SAN is attributed to the improved interfacial adhesion. According to Majumdar et al. [27,28], a reduction in the dispersed phase size and the presence of a compatibiliser at the interface broadens the interfacial region, which would translate on the macro-scale into higher ultimate strength.

3.4. Melt-mixed blends

The various SAN incorporated PS/NBR blends showed similar processing profiles during their melt-mixing, except the torque developed towards the end of melt-mixing. The steady torque values developed during the end of melt-mixing of PS/NBR/SAN systems are given in Table 7. The compatibilised blends show a higher steady torque than the uncompatibilised ones, due to the emulsifying action of SAN at the interfaces and the possible occurrence of micelle formation. The PS_{30} and PS_{50} compatibilised blends show

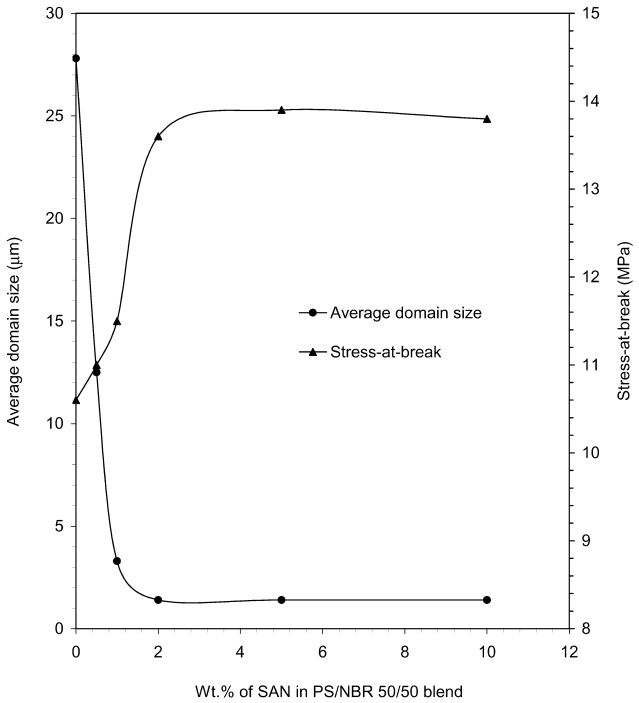

Fig. 9. Variation of reduction in domain size and stress-at-break as a function of SAN concentration in solution-casted PS_{50} blend.

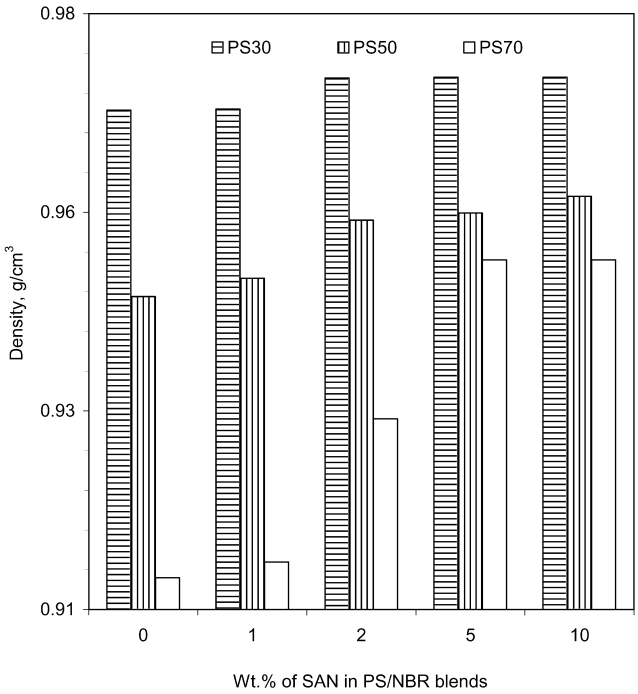

Fig. 10. Variation of density as a function of SAN concentration in PS/NBR blends.

higher steady torque due to the continuous nature of the high viscous NBR phase. The densities of different SAN compatibilised PS/NBR blends are shown in Fig. 10. The incorporation of SAN marginally increases the density of the respective PS/NBR blend. The positive deviation of density from the additive contribution of respective components is caused due to the increased interfacial adhesion and consequent packing densification of the compatibilised blends [29].

Fig. 11 show the scanning electron micrographs of the cryogenically fractured surface of PS_{50} blends with 0, 2, 5 and 10 wt% SAN, respectively. In these blends, the PS-phase has been etched with cyclohexane, and hence the holes indicate the extracted phase. In the uncompatibilised PS_{50} blend, both the PS and NBR components tend to form the continuous phase. The phase co-continuity of PS_{50} blend is retained on addition of SAN copolymer in it. The morphology of the compatibilised blends shows that the addition of the copolymer results in a considerable reduction in the phase heterogeneity. Also, the blends attain a more uniform distribution of the PS and NBR components on compatibilisation.

Table 7 summarises the effect of the addition of SAN on the mechanical properties of melt-mixed PS/NBR blends.

Table 6
Mechanical properties of solution (chloroform) casted PS/NBR blends compatibilised with SAN copolymer

Sample	Young's modulus (MPa)	Stress-at-break (MPa)	Break-strain (%)	Tear strength (N/mm)
$PS_{30}S_0$	6.7 ± 2.3	3.5 ± 0.6	131 ± 11	13.9 ± 0.1
$PS_{30}S_1$	7.3 ± 2.2	4.1 ± 0.5	135 ± 9.0	17.0 ± 0.2
$PS_{30}S_2$	8.1 ± 1.6	5.9 ± 0.3	146 ± 2.6	21.3 ± 0.4
$PS_{30}S_5$	8.2 ± 1.8	5.8 ± 0.4	146 ± 3.2	21.5 ± 0.3
$PS_{30}S_{10}$	8.8 ± 1.3	5.9 ± 0.3	149 ± 2.2	21.8 ± 0.3
$PS_{50}S_0$	80.6 ± 7.0	10.6 ± 0.6	40.5 ± 2.5	52.3 ± 0.2
$PS_{50}S_1$	115 ± 15	11.5 ± 0.2	42.1 ± 1.6	56.3 ± 0.3
$PS_{50}S_2$	140 ± 7.6	13.6 ± 0.1	44.5 ± 0.8	62.5 ± 0.2
$PS_{50}S_5$	139 ± 8.2	13.6 ± 0.2	44.6 ± 0.5	62.9 ± 0.5
$PS_{50}S_{10}$	141 ± 5.3	13.8 ± 0.1	45.8 ± 0.3	62.4 ± 0.8
$PS_{70}S_0$	240 ± 10	19.2 ± 0.8	19.5 ± 0.5	74.3 ± 0.6
$PS_{70}S_1$	313 ± 8.4	23.2 ± 0.8	23.2 ± 0.2	78.2 ± 0.2
$PS_{70}S_2$	564 ± 8.4	26.3 ± 0.6	26.7 ± 0.2	83.4 ± 0.2
$PS_{70}S_5$	576 ± 6.0	26.0 ± 0.4	26.8 ± 0.1	83.1 ± 0.4
$PS_{70}S_{10}$	540 ± 13	25.8 ± 0.4	26.3 ± 0.1	84.1 ± 0.4

Values are mean ± standard deviation.

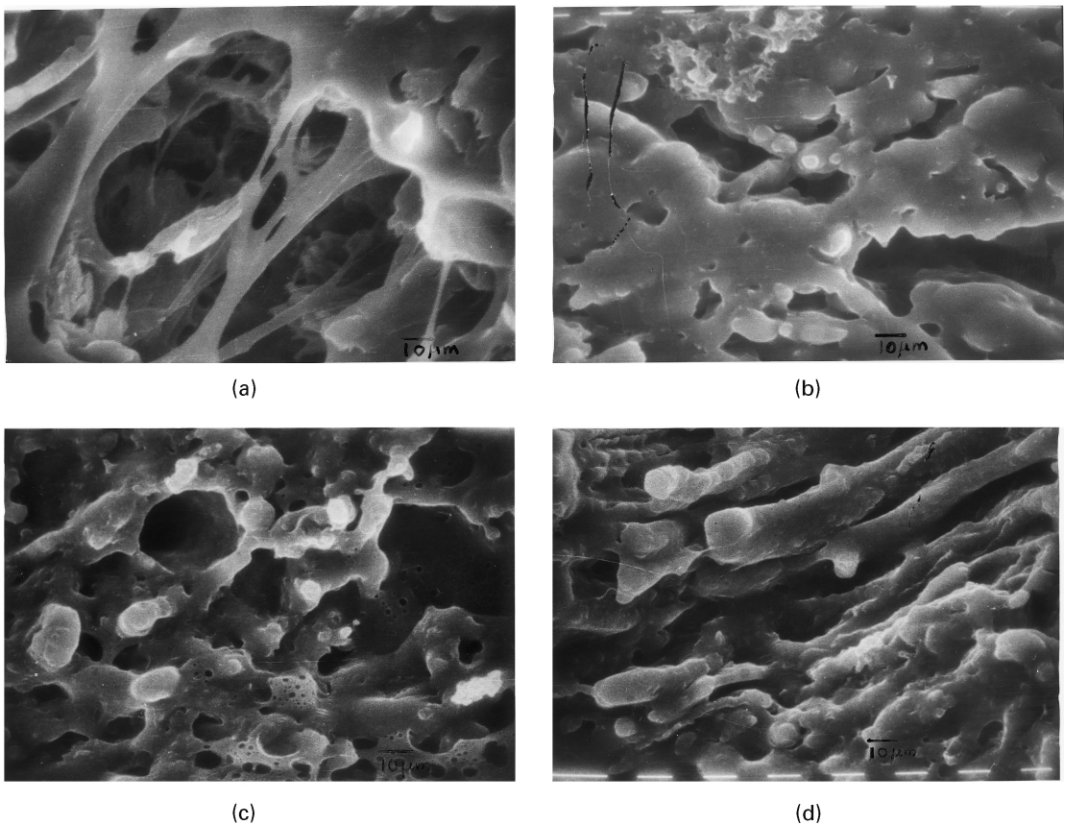

Fig. 11. SEM photomicrograph of melt-mixed PS_{50} blend with (a) 0% SAN; (b) 2% SAN; (c) 5% SAN; and (d) 10% SAN (Mag: 800 ×).

Addition of SAN in PS/NBR system improves the tensile modulus of the blends. The increase in tensile modulus with the addition of SAN is due to the enhancement in interfacial adhesion between NBR and PS phases. For PS_{70} and PS_{50} blends, the highest tensile modulus is obtained at 5 wt% SAN concentration, while the lowest value is obtained for the uncompatibilised blends. Also, addition of SAN in PS_{70} blend brings about a higher increase in modulus compared to PS_{50} and PS_{30} blends. This may be explained as follows: since SAN is a random copolymer, it cannot penetrate deep into the phases, and rather, concentrates more at the interface. This leads to substantial increase in interfacial

Table 7
Mechanical properties of melt-mixed PS/NBR blends compatibilised with SAN copolymer

Sample	Steady torque[a] (Nm)	Young's modulus (MPa)	Stress-at-break (MPa)	Break-strain (%)	Tear strength (N/mm)	Notched Izod impact strength (J/m)	Hardness (shore D)
$PS_{30}S_0$	10.3	3.6 ± 1.6	1.3 ± 0.3	119 ± 11	7.9 ± 0.1	514 ± 2.9	23
$PS_{30}S_1$	10.5	4.8 ± 2.0	1.8 ± 0.5	119 ± 9.0	8.0 ± 0.2	794 ± 1.6	26
$PS_{30}S_2$	10.8	6.2 ± 1.4	2.1 ± 0.3	133 ± 2.6	8.9 ± 0.4	865 ± 8.8	28
$PS_{30}S_5$	10.6	6.4 ± 0.8	2.3 ± 0.4	127 ± 3.2	9.5 ± 0.3	807 ± 6.6	31
$PS_{30}S_{10}$	10.6	6.7 ± 1.2	1.9 ± 0.2	127 ± 2.2	9.8 ± 0.3	848 ± 4.0	31
$PS_{50}S_0$	8.6	50.6 ± 17	5.5 ± 0.6	21.8 ± 2.5	39.5 ± 0.2	625 ± 18	50
$PS_{50}S_1$	8.7	75.0 ± 15	6.1 ± 0.2	23.1 ± 1.6	40.0 ± 0.3	841 ± 11	51
$PS_{50}S_2$	9.0	109 ± 7.6	7.8 ± 0.3	27.0 ± 0.8	42.2 ± 0.2	936 ± 6.6	55
$PS_{50}S_5$	9.0	115 ± 8.2	6.9 ± 0.2	29.3 ± 0.5	47.9 ± 0.5	919 ± 4.5	57
$PS_{50}S_{10}$	9.3	110 ± 5.3	6.8 ± 0.1	29.9 ± 0.3	47.2 ± 0.8	938 ± 4.0	59
$PS_{70}S_0$	6.3	125 ± 10	14.2 ± 0.8	9.8 ± 0.5	56.3 ± 0.6	110 ± 2.5	71
$PS_{70}S_1$	6.3	340 ± 1.2	17.6 ± 0.8	15.4 ± 0.2	59.2 ± 0.2	145 ± 1.6	72
$PS_{70}S_2$	6.5	550 ± 6.1	20.9 ± 0.6	16.3 ± 0.2	63.6 ± 0.2	553 ± 1.0	74
$PS_{70}S_5$	6.6	570 ± 4.4	21.0 ± 0.4	16.1 ± 0.1	69.3 ± 0.4	418 ± 0.8	74
$PS_{70}S_{10}$	6.6	499 ± 20	20.5 ± 0.4	16.0 ± 0.1	68.3 ± 0.4	407 ± 2.8	75

Values are mean ± standard deviation.
[a] Equilibrium torque value at the end of the melt-mixing process.

thickness. This effect is more pronounced in PS_{70} system where the rubber (NBR) phase is dispersed in the continuous low viscosity PS matrix. In fact, the addition of SAN copolymer suppresses the coalescence of the NBR phase leading to fine particle size. In the absence of the random copolymer, the coalescence is severe in PS_{70} because the rubber particles can undergo shear induced aggregation in the low viscosity PS phase. Incorporation of SAN in PS_{70} suppresses this considerably. Both the above factors contribute to the substantial increase in the ultimate strength of PS_{70} with compatibilisation. The stress-at-break (σ_b) values of the compatibilised compositions is higher than the uncompatibilised ones. With the addition of the compatibiliser, the interfacial condition of the blend is improved, thereby increasing its tensile strength. The PS_{30} blends showed only a marginal increase with the SAN concentration. The tensile strength improvement is more in the case of PS_{70} system. A levelling-off in tensile strength can be observed at 2–5 wt% SAN concentration in the blends. The levelling-off in σ_b values in the blends can be correlated with the saturation of SAN molecules at the PS/NBR interface. In all the three blends, the compatibilised compositions are more ductile than the uncompatibilised ones. For example, the uncompatibilised PS_{70} shows low break-strain (9.8%). Addition of 5 wt% SAN in the blend increases the break-strain to 16%. The increase in ductility of PS/NBR blends with compatibilisation is due to the improved interfacial adhesion. An improvement in elongation-at-break on compatibilisation of polymer blends has been reported in literature [30,31]. Addition of SAN in PS/NBR improves the tear strength of the blend. The change in tear strength of the blends can be explained in terms of the change in morphology with compatibilisation. With increasing concentration of SAN in the blend, the average dispersed phase size decreases and the number of deformable particles per unit area increases proportionally. The highly deformable particles in the compatibilised systems are able to elongate to the high strain-levels and obstruct the advancing tear front more effectively. The tear strength of blends are considerably higher when the NBR particles comprise the dispersed phase (i.e. PS $\geq$ 50 wt%). As in the case of tensile properties, the levelling-off observed in tear strength at 5 wt% SAN is also due to the interfacial saturation. Although, hardness is a surface property, the compatibilising effect of SAN shows an increase in shore hardness of PS/NBR blends. Perhaps, the particle size reduction and accompanying packing densification contributes to the enhanced hardness.

The effect of compatibiliser concentration on the impact strength is given in Table 7. The uncompatibilised PS_{30} is, as such tough, having an impact strength of 514 J m^{-1}. The incorporation of just 1 wt% SAN increases the impact strength to 794 J m^{-1}. Increasing the compatibiliser concentration beyond 2 wt% results in a plateau effect. The PS_{50} blends also show a similar behaviour as that of PS_{30} blends. Since PS matrix (without rubber) is very brittle, the PS_{70} blend expectedly shows poor impact toughness. Addition of SAN increases the toughness of the brittle blend by a factor of 3–5. This is a significant improvement, with the brittle blend exhibiting considerable toughness at an optimum concentration of 2 wt% SAN. Both large particle-size and weak adhesion appear to have caused the deterioration in impact properties and resulting brittleness of uncompatibilised PS_{70}. On the other hand, the compatibilised PS_{50} and PS_{30} blends have notched impact toughness of 806–936 J m^{-1} with an improvement of 70% over the corresponding uncompatibilised blends, and they are transformed to super tough materials in impact. The impact results indicate the importance of a critical SAN concentration for toughening of PS/NBR blends. The particle size must be smaller than the critical size to achieve a tough behaviour [31]. As discussed earlier, the reduction in particle size was obtained by the addition of 2–5 wt% SAN in the blends, and this was found to be sufficient to effectively saturate the PS/NBR interface. The effect of increasing the concentration of SAN beyond 2–5 wt% would only be to force away a portion of it away from the blend interface, to form micellar aggregates in the matrix. It is expected that such a situation would lead to an increased effective viscosity of the matrix. Thus, the incorporation of SAN above 5 wt% in PS/NBR does not improve the impact strength any further. Majumdar et al. [27,28] reported similar result on addition of imidized acrylic compatibiliser beyond 10 wt% in nylon-6/ABS system.

The PS/NBR systems present two extremes in properties, depending on whether the major component is plastic or rubber. When the blend is grossly PS-rich, we have strong ultimate properties but poor ductility. On the other extreme, the elastomeric NBR-rich blend has excellent elongational properties at the expense of ultimate strength. This section explores the minimum rubber concentration necessary for achieving a super-tough compatibilised blend, remaining reasonably ductile and mechanically strong. For this purpose, the SAN concentration is kept constant, while the PS content is varied. The stress–strain behaviour of the compatibilised PS/NBR blends can be analysed from Fig. 8(b). The PS_{50} blends show elastic and inelastic regions. In the case of PS_{30}, the modulus of the compatibilised blend is improved vastly relative to the uncompatibilised one. The PS_{70} blends show remarkable stiffness due to the presence of PS matrix. The higher tensile strength and modulus of PS_{70} and PS_{50} blends in comparison to PS_{30} blends is due to the continuous nature of PS phase and smaller particle sizes. Fig. 12 shows the Izod impact strength (notched) of PS/NBR blends, compatibilised as well as uncompatibilised. There is a drastic drop in the impact strength as the NBR concentration is decreased from 50 to 30%, corresponding to the critical NBR concentration for toughening of PS/NBR blends. The superior impact toughness of PS_{50} blends is associated with the co-continuous phase morphology in the blends. All the compatibilised blends, including PS_{70}, have impact strength in the range 407–936 J m^{-1}. It is evident

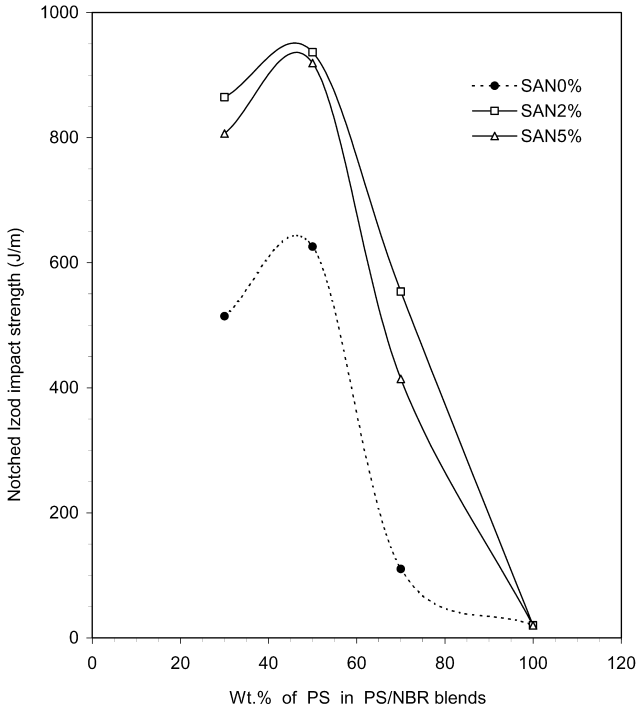

Fig. 12. Notched Izod impact strength of compatibilised PS/NBR blends as a function of blend composition.

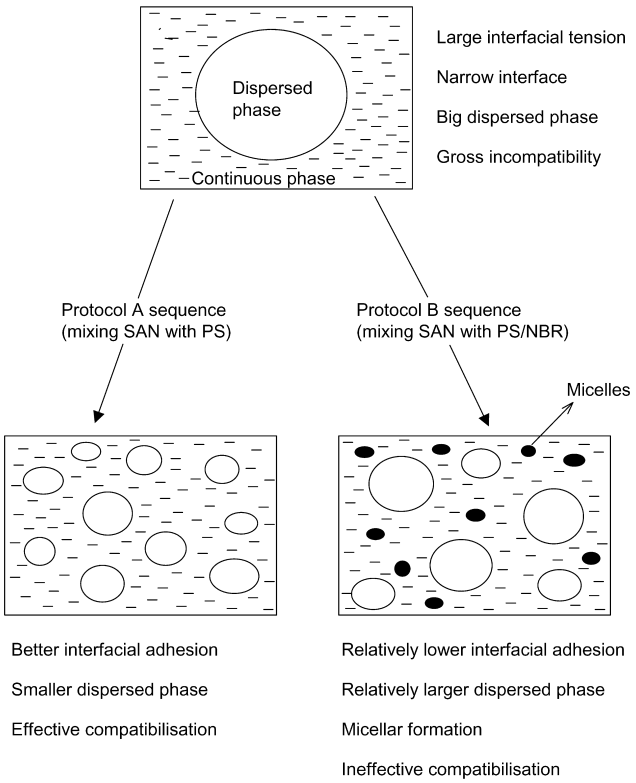

Fig. 13. Speculative model representing the behaviour of compatibiliser having different modes of mixing.

that super-tough materials can be achieved over a broad range of PS/NBR ratios, by addition of SAN copolymer. Thus, addition of 2–5 wt% SAN in PS/NBR gave blends with a more uniform phase distribution, lesser phase heterogeneity and improved ultimate strength than the uncompatibilised blends.

3.5. Effect of mixing protocol during melt-blending

The sequence of addition of the compatibiliser during mixing has been found to affect the blend properties [28,32,33]. Hence, the sensitivity of PS/NBR blends to the mode of addition of SAN copolymer was examined. Protocol (A) consisted of pre-blending PS with SAN, which was then blended with NBR in a second step. Protocol (B) consisted of first blending PS with NBR, followed by blending the mix with SAN in a second step. The sequence of mixing is shown schematically in Fig. 13. Table 8 summarises the results of the two different mixing protocols on the mechanical properties of the three blends. The blend properties are highly sensitive to the sequence of mixing. The protocol (A) mixed blends showed superior tensile properties than those prepared as per protocol (B). The tear strength also showed a similar behaviour. The impact toughness of the blends showed higher values when SAN was incorporated as per protocol (A). The impact strength of the blends prepared with protocol (B) dropped by as much as 31–34% for the compatibilised compositions with respect to the protocol (A) mixed blends. The impact strength of blends is greatly dependent upon the capacity of dissipating impact energy through the matrix and the transfer of the internal stress of the continuous phase to the dispersed phase [31]. Hence, the interfacial condition between the phases is very important. The speculative model in Fig. 13 suggests that mixing as per protocol (A)

Table 8
Effect of the mode of addition of SAN copolymer during melt-blending on the PS/NBR blend properties

Mechanical properties	$PS_{30}S_2$ blend		$PS_{50}S_2$ blend		$PS_{70}S_2$ blend	
	Protocol (A) mix	Protocol (B) mix	Protocol (A) mix	Protocol (B) mix	Protocol (A) mix	Protocol (B) mix
Young's modulus (MPa)	6.2	5.7	109	84.0	550	538
Stress-at-break (MPa)	2.1	1.6	7.8	6.7	20.9	18.4
Break-strain (%)	133	127	27	20	16	15
Tear strength (N/mm)	8.9	8.3	42.2	40.8	63.6	61.5
Notched Izod impact strength (J/m)	865	568	936	870	553	378

would locate the compatibiliser at the interface in a more efficient manner. In protocol (A) blending, owing to the low melt viscosity of PS and SAN, it would form a homogeneous melt. The subsequent melt-mixing of this pre-blend with NBR would result in stronger adhesion between PS/NBR interface. However, mixing as per protocol (B) would inhibit the mobility of the compatibiliser towards the already formed interface and retard the emulsifying phenomenon of the interface. Thus, adding the compatibiliser as per protocol (A) would result in better interfacial adhesion in the blend. However, the morphology of the blends prepared as per protocol (A) did not show any notable differences with respect to that prepared as per protocol (B). The effect of the mode of compatibiliser addition on the blend properties was higher when the plastic component was the dispersed phase. The mechanical properties of PS_{30} and PS_{50} blends showed large difference when the mode of compatibiliser addition was changed. But, properties of PS_{70} blend were less affected by the change in mixing sequence. This is due to the high viscosity of the continuous phase in the NBR-rich blends. The viscosity ratio of NBR with respect to SAN is 1.56 ($= \eta_{NBR}/\eta_{SAN}$) while the viscosity ratio of PS with respect to SAN is 0.69 ($= \eta_{PS}/\eta_{SAN}$). Hence, the mobility of SAN would be affected by the nature of the continuous phase of the blend. The mobility of the compatibiliser molecule would be lower in blends in which NBR is the continuous phase and its location at the interface would be increasingly difficult. Willis and Favis [32] and Asalata et al. [33] have reported that the two-step mixing is more effective in reducing the dispersed phase size than the one-step mixing during compatibilisation. In the case of PS_{30} and PS_{50}, by pre-blending SAN with PS (i.e. the dispersed phase in the blend), the amount of copolymer that can diffuse into the interface can be increased and the distance travelled by the copolymer to reach the interface can be minimised. This will lead to the preferential location of the SAN copolymer at the PS/NBR interface during mixing and result in higher interfacial adhesion. Thus, compared to one-step mixing (Protocol-B), in two-step mixing (Protocol-A), the amount of compatibiliser diffusing into the interface is increased and the distance travelled by the compatibiliser to reach the blend interface is minimised. This leads to better interfacial interaction of the compatibiliser and facilitates the most efficient combination of mechanical properties.

4. Conclusions

Owing to the poor interfacial adhesion and bigger particle size of the dispersed phase, PS/NBR binary blends have poor mechanical properties. In this work, the possibility of compatibilising PS/NBR blends using SAN was explored. The influence of compatibilisation on the morphology and mechanical properties of the blends has been studied. The incorporation of SAN is effective in reducing the phase size of PS/NBR blends. The domain size of the dispersed phase decreases with the addition of small amount of the copolymer, followed by levelling-off at higher concentration. The experimental result is found to be in agreement with the theoretical predictions of Noolandi and Hong. The CMC of the compatibiliser required to saturate the PS/NBR interface was determined for different blend compositions. The studies on solution-casted blends reveal that 1–2 wt% of SAN is sufficient to effectively saturate the interface of PS/NBR blends. In optimally compatibilised system, the presence of the copolymer layer between the aggregated domains inhibits coalescence and narrows the particle size distribution. The Young's modulus, tensile strength and tear strength are substantially improved by the addition of SAN copolymer in solution-casted as well as melt-mixed PS/NBR blends. The properties attain an optimum value when the reduction in domain size is maximum. The blends show improved impact toughness upon compatibilisation. The compatibilised PS/NBR (50/50) and (70/30) compositions show an improvement of 70% in impact strength, and are transformed into super-tough materials. Varying the mixing protocol affected the key mechanical properties of melt-mixed blends. The effectiveness of the copolymer in enhancing the tensile properties increases when the plastic phase is continuous. The overall improvement in properties suggest that random SAN copolymer can be used as an effective compatibiliser in PS/NBR blends.

Acknowledgments

One of the authors (MM) acknowledges the financial support (research fellowship) from University Grants Commission, New Delhi for carrying out this research programme.

References

[1] Bhowmick AK, Stephens HL. Handbook of elastomers: new developments and technology. New York: Marcel Dekker; 1988. Chapter 5.
[2] Walker BM. Handbook of thermoplastic elastomers. New York: Van Nostrand Reinhold; 1979. Chapter 1.
[3] Utracki LA. Polymer alloys and blends. Munich: Hanser; 1989. Chapter 1.
[4] Hay D, Pfisterer HA, Storey EB. Rubb Age 1955;94:77–80.
[5] Fegade NB, Phondke NA, Millns W. Proc Int Rubb Conf 93, New Delhi 1993;43.
[6] Kumar CR, George KE, Thomas S. J Appl Polym Sci 1996;61:2383–96.
[7] Mathew M, Ninan KN, Thomas S. Polymer 1998;39:6235–41.
[8] Olabisi O, Robeson LM, Shaw MT. Polymer–polymer miscibility. New York: Academic Press; 1979. Chapter 5.
[9] Molau GE. J Polym Sci 1965;A3:4235–42.
[10] Molau GE. J Polym Sci 1965;B3:1007–15.
[11] Riess G, Kohler J, Tournut C, Banderet A. Makromol Chem 1967;101:58–73.

[12] Grindstaff TH, Patterson HT, Bilica HR. Chem Spec Mfr Assoc, Mid-year Meet 1969;55:110–4.
[13] Gaillard P, Ossenbach MS, Riess G. Makromol Chem Rapid Commun 1980;1:771–4.
[14] Fayt R, Jerome R, Teyssie P. J Polym Sci, Polym Phys Ed 1982;20: 2209–17.
[15] Fayt R, Jerome R, Teyssie P. Polym Engng Sci 1987;27:328–34.
[16] Thomas S, Prud'homme RE. Polymer 1992;33:4260–8.
[17] Leibler L. Makromol Chem, Macromol Symp 1985;16:17–21.
[18] Leibler L. Macromolecules 1982;15:1283–7.
[19] Noolandi J, Hong KM. Macromolecules 1982;15:482–92.
[20] Noolandi J, Hong KM. Macromolecules 1984;17:1531–7.
[21] Jannasch P, Wesslen B. J Appl Polym Sci 1995;58:753–70.
[22] Mathew M, Ninan KN, Thomas S. J Appl Polym Sci 2002; communicated.
[23] Tang T, Huang B. Polymer 1994;35:281–5.
[24] Paul DR, Newman S. Polymer blends. New York: Academic Press; 1978. Chapter 12.
[25] Heikens D. Kem Ind 1982;31:165–7.
[26] Plochocki AP, Dagli SS, Andrews RD. Polym Engng Sci 1990;30: 741–52.
[27] Majumdar B, Keskkula H, Paul DR. Polymer 1994;35:5453–67.
[28] Majumdar B, Keskkula H, Paul DR. Polymer 1994;35:5468–77.
[29] Ahn TO, Kim JH, Jeong HM, Lee SW, Park LS. J Polym Sci, Polym Phys Ed 1994;32:21–35.
[30] Chen G, Yang J, Liu JJ. J Appl Polym Sci 1999;71:2017–25.
[31] Bucknall C. Toughened plastics. London: Applied Science Publishers; 1977.
[32] Willis JM, Favis BD. Polym Engng Sci 1988;28:1416–26.
[33] Asalata R, Kumaran MG, Thomas S. Rubb Chem Technol 1995;68: 671–87.